Self-Propagating High-Temperature Synthesis
Самораспространяющийся высокотемпературный синтез

UDC 621.762 : 621.777 + 620.178.15 + 544.45
https://doi.org/10.17073/1997-308X-2025-6-16-26

Research article
Научная статья

Influence of mechanical activation of titanium and boron on the densification and combustion of Ti + 2B powder mixtures

Yu. V. Bogatov, **V. A. Scherbakov**

Merzhanov Institute of Structural Macrokinetics and Materials Science of the Russian Academy of Sciences
8 Akademican Osip'yan Str., Chernogolovka, Moscow Region 142432, Russia

xxbroddy@gmail.com

Abstract. The influence of mechanical activation (MA) of titanium and boron powders in a ball mill on the combustion behavior of Ti + 2B mixtures has been investigated. Experimental dependences of the combustion temperature and combustion-wave velocity on the density of compacts prepared from starting and mechanically activated powders were obtained. It was shown that the dependences of these parameters on the compact density exhibit pronounced maxima. With increasing density, the rise in combustion temperature is governed by the growth of the Ti–B reaction-interface area, whereas its subsequent decrease is associated with an increase in the Ti–Ti contact area. Mechanical activation exerts opposite effects on the reactants: it reduces the specific surface area of titanium powder, thereby decreasing the Ti–B contact area, but at the same time destroys the arch-like structure of amorphous boron and disperses its agglomerates, which increases the reaction-interface area. The overall result is an increase in the maximum combustion temperature to 2900 °C. It was experimentally established that, at compaction pressures above 30 MPa, mechanically activated boron exhibits limited plasticity, enabling consolidation of Ti + 2B mixtures to relative densities of 0.7–0.8. A correlation was found between electrical resistivity and combustion temperature: the highest combustion temperatures correspond to a resistivity range of $R \approx 10^{5.0} – 10^{5.5}$ Ω·cm, while a further decrease in resistivity – related to the growth of the Ti–Ti contact area – leads to a reduction in the combustion temperature.

Keywords: mechanical activation, titanium and boron powders, powder properties, compaction, Ti + 2B reactive mixture, combustion temperature, combustion-wave velocity

For citation: Bogatov Yu.V., Scherbakov V.A. Influence of mechanical activation of titanium and boron on the densification and combustion of Ti + 2B powder mixtures. *Powder Metallurgy and Functional Coatings*. 2025;19(6):16–26.
https://doi.org/10.17073/1997-308X-2025-6-16-26

Влияние механической активации титана и бора на уплотнение и горение смесей Ti + 2B

Ю. В. Богатов, **В. А. Щербаков**

Институт структурной макрокинетики и проблем материаловедения им. А.Г. Мержанова РАН
Россия, 142432, Московская обл., г. Черноголовка, ул. Акад. Осипьяна, 8

xxbroddy@gmail.com

Аннотация. В работе исследовано влияние механической активации (МА) порошков титана и бора в шаровой мельнице на процесс горения в композиции Ti + 2B. Получены экспериментальные зависимости температуры и скорости горения шихтовых образцов, спрессованных из исходных и активированных реагентов. Показано, что зависимости этих параметров от плотности прессованных образцов имеют ярко выраженный максимум. Установлено, что с ростом плотности шихтовых прессовок повышение температуры горения обусловлено увеличением площади контакта между частицами титана и бора (Ti–B), а ее снижение – с увеличением площади контакта между частицами титана (Ti–Ti). Установлено, что МА оказывает разнонаправленное действие на реагенты: она снижает удельную поверхность порошка Ti, уменьшая площадь

контакта Ti–B, но одновременно разрушает аморфную структуру бора, диспергируя его агломераты, что увеличивает реакционную поверхность. Результирующим эффектом является повышение максимальной температуры горения до 2900 °C. Экспериментально обнаружено, что при уплотнении выше давления 30 МПа порошок бора после МА способен проявлять пластические свойства, что позволило консолидировать порошковые смеси Ti + 2B до плотности 0,7–0,8. Обнаружена корреляция между уровнем электрического сопротивления и температурой горения: максимальные значения температуры горения соответствовали уровню удельного электросопротивления шихтовых прессовок $R \approx 10^{5,0} – 10^{5,5}$ Ом·см, ниже которого температура горения снижалась, что связано с увеличением площади контактной поверхности между частицами титана.

Ключевые слова: механическая активация, свойства порошков титана и бора, прессование, реакционная смесь Ti + 2B, температура и скорость горения

Для цитирования: Богатов Ю.В., Щербаков В.А. Влияние механической активации титана и бора на уплотнение и горение смесей Ti + 2B. *Известия вузов. Порошковая металлургия и функциональные покрытия*. 2025;19(6):16–26. https://doi.org/10.17073/1997-308X-2025-6-16-26

Introduction

Titanium diboride, owing to its unique properties – including ultrahigh melting point, high hardness, and strong neutron absorption capability – is widely used in mechanical engineering, metallurgy, and the nuclear industry [1–7]. A promising route for producing dense TiB_2 ceramics is SHS compaction (SHS – self-propagating high-temperature synthesis) [8; 9]. However, achieving high-density TiB_2 ceramics by this method is challenging due to the insufficiently developed stage of preparing the reactive mixtures prior to synthesis. Earlier studies on obtaining dense TiB_2 focused primarily on combustion processes [10–15] and hot pressing of reaction products [16; 17]. In contrast, the preparatory treatment of reactive mixtures received limited attention, despite its substantial influence on combustion parameters, morphology, microstructure, and ceramic properties [18; 19].

It was shown in [20] that mechanical activation of the reactants increases the combustion temperature, enhances structural integrity, and reduces both residual porosity and TiB_2 grain size. Our earlier works [18; 19] demonstrated that the combustion temperature (T_c) of Ti + 2B mixtures can be increased to the adiabatic level (3190 °C [20]) by increasing the reaction interface between titanium and boron particles. The main technological approaches for increasing T_c included selecting titanium powders with a high specific surface area (1.0–1.5 m^2/g) [18] and mechanical activation of the reactants during mixing [19].

Despite these positive results, several issues concerning the conditions for preparing the reactive mixtures and the mechanisms by which these conditions affect combustion behavior remain unresolved. Changes in the characteristics of the reactants during mechanical treatment in a ball mill, as well as during compaction, and the influence of these changes on combustion parameters have not been sufficiently investigated.

The aim of the present work was to study the influence of mechanical activation of the initial reactants – titanium and boron – on the physical and technological properties and combustion behavior of Ti + 2B powder mixtures.

Materials and methods

Titanium powder grade PTM (TU 14-22-57-92) and amorphous boron powder (TU 113-12-132-83) were used in the experiments. Their characteristics – including the content of main components, oxygen and hydrogen levels, bulk density (Θ_b), tap density (Θ_t), and particle-size distribution (d) – are presented in Table 1.

Mechanical activation of the starting powders was performed in a 2.5 L ball mill at a drum rotation speed of 60 rpm, with a charge-to-ball mass ratio of M_{ch}/M_{ball} = 1:15. The milling media were ShKh15 bearing steel balls, 25 mm in diameter. Titanium and boron powders were mixed in the stoichiometric molar ratio Ti + 2B, corresponding to the following mass

Table 1. **Characteristics of the powder reactants**

Таблица 1. **Характеристики порошковых реагентов**

Reactant	Composition, wt. %			Bulk density, Θ_b, rel. units	Tap density, Θ_t, rel. units	d, μm
	Main component	[O]	[H]			
Ti	97	0.6	0.3	0.32	0.35	<50.0
B	93	4.1	0.6	0.14	0.21	<0.2

fractions in the mixtures: 69 wt. % Ti and 31 wt. % B. Mixtures were prepared using both the initial powders (Ti_{ini} and B_{ini}), and powders mechanically activated in the ball mill – titanium for 40 h (Ti_{MA}) and boron for 30 h (B_{MA}).

To avoid introducing uncontrolled changes in the powder characteristics during mixing, all mixtures were prepared by manual blending in a ceramic mortar. In total, four mixtures were obtained: *1* – ($Ti_{исх}$ + 2B_{ini}), *2* – (Ti_{MA} + 2B_{ini}), *3* – (Ti_{ini} + 2B_{MA}) and *4* – (Ti_{MA} + 2B_{MA}).

The bulk density (Θ_b) was measured according to GOST 19440-94 (ISO 3923-1-79), and the tap density (Θ_t) according to GOST 25279-93 (ISO 3953-85). Each value represents the average of 3–5 measurements. The relative increase in density after tapping was calculated as

$$\Delta\Theta_t = \frac{\Theta_t - \Theta_b}{\Theta_b} \cdot 100\ \%.$$

The relative density of the mixture was calculated using the densities of titanium (4.5 g/cm^3), amorphous boron (1.8 g/cm^3), and the theoretical density of the Ti + 2B mixture (3.08 g/cm^3).

The specific surface area of the powders was evaluated using nitrogen adsorption (BET method). The relative measurement uncertainty did not exceed 6 %. Titanium (25 g), boron (15 g), and their reactive mixtures (20 g) were compacted in a 30-mm die at pressures of 5–170 MPa to achieve a relative density of 0.50–0.88. Axial elastic springback after unloading was measured in accordance with GOST 29012-91 (ISO 4492-85).

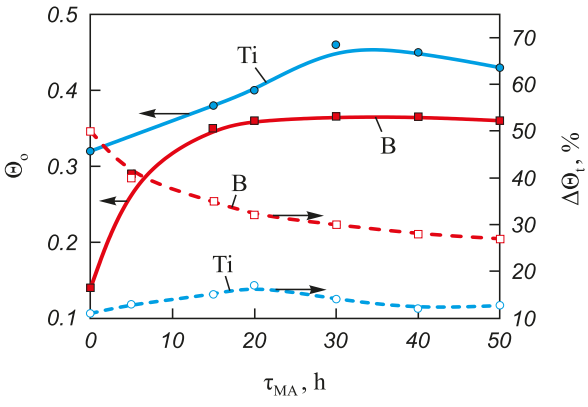

Fig. 1. Dependance of bulk density and change in tap density on mechanical activation time for Ti and B powders

Рис. 1. Зависимости насыпной плотности и изменение плотности при утряске от времени МА для порошков Ti и B

The electrical resistance (R) of the pressed samples (30 mm in diameter, 10–15 mm in height) was measured by a two-point method using a V7-40/4 digital voltmeter. Sample height served as the measurement baseline.

The maximum combustion temperature (T_{max}) and the average combustion front velocity (U_c) were determined using 200 μm tungsten–rhenium thermocouples following the methodology described in [18]. Thermocouple signals were recorded with an analog-to-digital converter and stored on a computer; the sampling frequency was 1 kHz. The reported combustion temperature and combustion velocity values represent the average of three experiments. The measurement error did not exceed 3 %.

Experimental results

Mechanical activation of titanium and boron powdera

Important characteristics of powders are the bulk density and the relative increase in density on tapping, which are governed by interparticle friction and depend on particle shape and surface roughness [21]. Their variation with mechanical activation time MA (Fig. 1).

Initially, titanium particles have a dendritic, sponge-like morphology with both open and closed porosity (Fig. 3, *a*), and a bulk density of Θ_b = 0.32. The smooth particle surface results in a minimal increase in density on tapping ($\Delta\Theta_t$ = 11 %). During treatment with the grinding media, fragmentation and smoothing of the Ti particle shape occur. In the first stage of mechanical activation (up to 20 h), two processes proceed simultaneously: milling-induced fragmentation of large sponge-like titanium particles and rounding of dendritic particles. The first process leads to a more uniform distribution of the smaller fragments between the larger particles, an increase in bulk density, and an increase in the specific surface area S_{sp} of the titanium powder (Fig. 2). The resulting irregular, angular fragments have a more defective surface compared to the starting particles, which increases $\Delta\Theta_t$ to 17 %. The second process – rounding of the Ti particles – also increases the bulk density but reduces the specific surface area of the particles. As a result, in the first stage (0–20 h of MA) the value of S_{sp} emains almost unchanged, while Θ_b and $\Delta\Theta_t$ increase (Fig. 1).

Figure 2 also shows the evolution of the electrical resistivity (R) of the titanium powder as a function of mechanical activation time. The higher initial resistivity of the starting titanium powder ($R \approx 10^{8.5}$ Ω·cm) is associated with the presence of an oxide film on

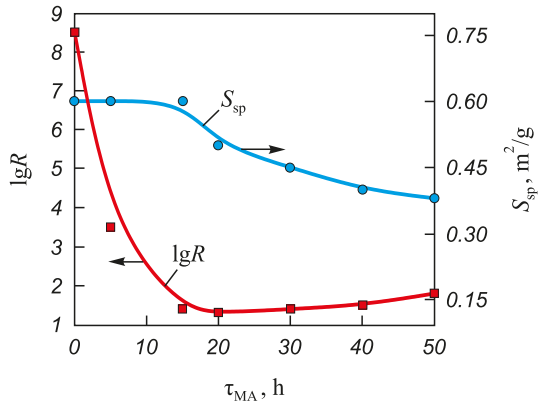

Fig. 2. Dependance of specific surface area and electrical resistivity of titanium powder on mechanical activation time

Рис. 2. Зависимости удельной поверхности и удельного электросопротивления порошка титана от времени МА

the Ti particle surface. During 5–15 h of MA this film is destroyed, which increases the true contact area between titanium particles and reduces the resistivity to $R \approx 10^{1.5}$ Ω·cm. Fragmentation of the large sponge-like Ti particles is essentially completed after 20–30 h of MA. Rounding of the titanium particles and smoothing of their shape continue, accompanied by an intensive increase in the number of surface defects (Fig. 3, *c*). As a result, the powder characteristics deteriorate: Θ_b decreases from 0.46 to 0.43, $\Delta\Theta_t$ decreases to 13 %, S_{sp} decreases to 0.35 m²/g, while R increases to $\approx 10^{1.9}$ Ω·cm in the interval from 20 to 50 h of MA (Fig. 2). This behavior is attributed to a decrease in the real contact area between titanium particles (see Fig. 1) caused by the increased defectiveness of the particle surfaces (Fig. 3, *c*).

The starting boron powder forms an arch-like packing structure, which is easily destroyed during tapping. This arching effect is associated with the formation of pores in the powder bed whose dimensions exceed the size of the largest particles. Such a packing structure results in a low bulk density of boron ($\Theta_b = 0.14$) and a high relative increase in density on tapping ($\Delta\Theta_t = 50$ %) (see Fig. 1). The starting powder contains agglomerates 1–2 μm in size composed of individual boron particles 0.1–0.3 μm in diameter (Fig. 4, *a*). As shown in our measurements, the specific surface area remains practically unchanged during interaction with the steel balls, staying within 8–9 m²/g. However, the tendency to form arch-like

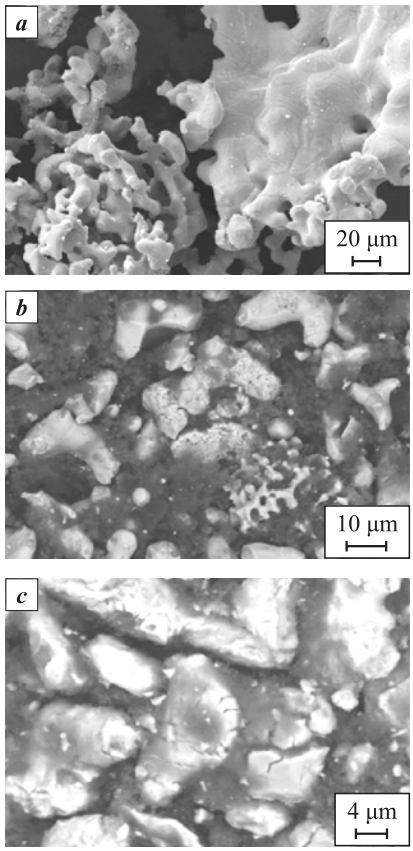

Fig. 3. Micrographs of the starting titanium powder (***a***) and after 20 h (***b***) and 50 h of (***c***) of mechanical activation

Рис. 3. Микрофотографии исходного порошка титана (***a***) и после МА 20 ч (***b***) и 50 ч (***c***)

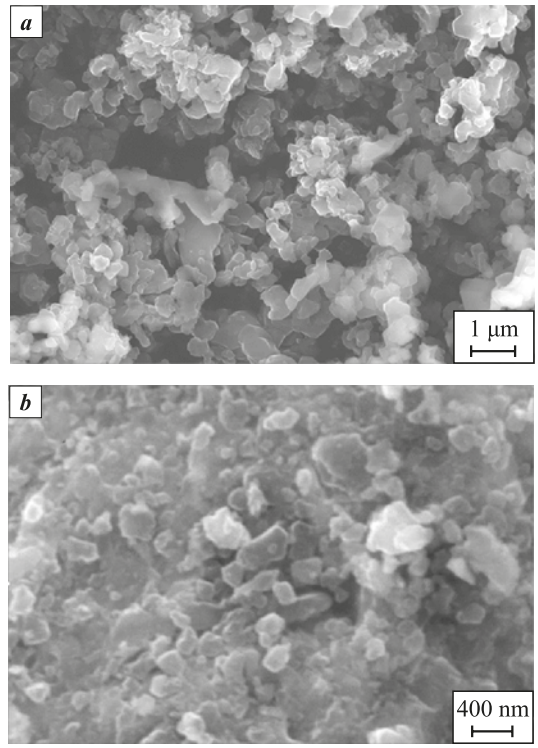

Fig. 4. Micrographs of the starting boron powder (***a***) and after mechanical activation (***b***)

Рис. 4. Микрофотографии исходного порошка бора (***a***) и после МА (***b***)

structures decreases, and the agglomerates of boron particles are gradually destroyed (Fig. 4, *b*), which reduces $\Delta\Theta_t$ to 27 % and increases Θ_b to 0.37 (Fig. 1). Individual boron particles 0.2–0.3 μm in size are visible in Fig. 4, *b*.

Compaction of elemental powders and their mixtures

Powder densification is conventionally divided into three stages [21; 22]: structural, elastic, and plastic deformation. For real powder systems this classification is approximate, and in practice the transition from structural deformation to elastoplastic deformation is usually gradual. Fig. 5 shows the dependence of density, axial elastic springback, and specific electrical resistivity of titanium compacts on the applied pressure. The compaction curve of mechanically activated titanium lies above that of the starting powder (Fig. 5, *a*). This behavior is explained by the higher bulk density of Ti_{MA} (Θ_b = 0.45), compared with Ti_{ini} (Θ_b = 0.32).

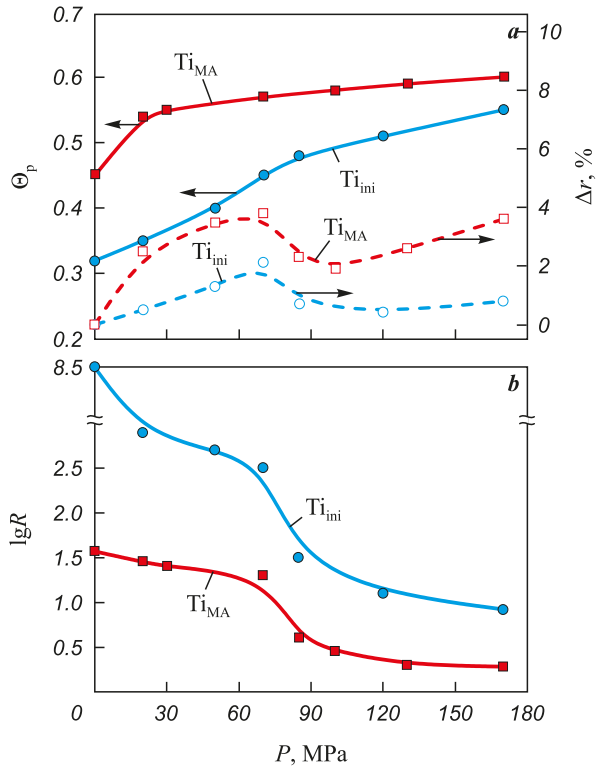

Fig. 5. Dependence of relative density and axial elastic springback (***a***), and specific electrical resistivity (***b***), on the compaction pressure for the starting and mechanically activated titanium powders

Рис. 5. Зависимости относительной плотности, упругого последействия (***a***) и удельного электросопротивления (***b***) от давления прессования порошков исходного титана и после МА

One way to determine the onset of plastic deformation is to analyze the pressure dependence of axial elastic springback (Δr) together with the compaction curve. The appearance of elastic springback with increasing compaction pressure indicates that the structural deformation stage has ended and the elastoplastic deformation stage has begun. The initial increase in Δr is caused by the accumulation of elastic stresses at interparticle contacts, where the bonding strength is still low. As the applied pressure increases and exceeds the yield strength of the particles, the plastic deformation stage begins; at this stage Δr decreases because the rate of bond strengthening between particles becomes higher than the rate of elastic stress accumulation. With further pressure increase, Δr begins to rise again, as the rate of elastic stress build-up at contacts once more exceeds the rate of bond strengthening [21].

Figure 5, *a* shows the axial springback as a function of pressure for the starting and mechanically activated titanium powders. The plastic deformation stage, indicated by a decrease in Δr, begins above 85 MPa. The higher true contact area between Ti_{MA} particles compared with Ti_{ini} results in higher elastic stresses (elastic springback). The value of Δr is determined by the contact area between titanium particles, where these stresses are generated. The larger the contact area, the higher Δr at the same compaction pressure [21].

The contact surface area between particles determines the electrical conductivity of titanium powders. Within the investigated pressure range, the electrical resistivity of Ti_{MA} compacts is lower than that of Ti_{ini} (Fig. 5, *b*), due to the rounding of the particles during mechanical activation and the resulting increase in the true contact area. At the onset of the plastic deformation stage ($P \approx 85$ MPa), a pronounced decrease in lg$R$ is observed, which is associated with the accelerated growth of the interparticle contact area (Fig. 5, *b*).

Figure 6 shows the evolution of relative density and axial elastic springback as a function of compaction pressure for the starting and mechanically activated boron powders. The compactability of B_{MA} is higher than that of B_{ini}. The shape of the Δr curve for B_{MA} corresponds to curves typical of ductile powders, such as titanium (see Fig. 5, *a*). In the range P = 30–50 MPa, a decrease in Δr is observed for B_{MA}, indicating the onset of the plastic deformation stage. With further pressure increase above 60 MPa, the elastic springback of B_{MA} rises again, similar to the behavior observed for titanium powders.

The springback curve for B_{ini} lies above that for B_{MA}. This reflects the stronger elastic response of B_{ini} during compaction. Up to about 85 MPa (Fig. 6), the compaction energy is spent mainly on breaking

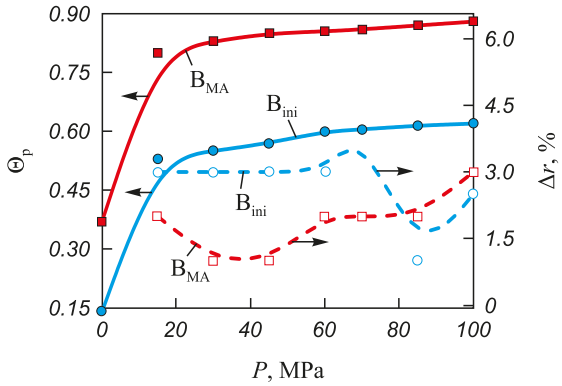

Fig. 6. Dependence of relative density and axial elastic springback on the compaction pressure for the starting and mechanically activated boron powders

Рис. 6. Зависимости относительной плотности прессовок и упругого последействия от давления прессования исходного порошка бора и после МА

the arches and agglomerates that define the structural packing of the starting boron powder. For this reason, the plastic deformation stage in B_{ini} begins later than in B_{MA}, at pressures exceeding 85 MPa.

Compaction of Ti + 2B mixtures

Titanium and boron powders – both starting and mechanically activated for 40 h (Ti_{MA}) and 30 h (B_{MA}), respectively – were used for preparing the mixtures. Since mixing in a ball mill may introduce uncontrolled changes in powder characteristics, the mixtures were blended manually in a ceramic mortar to avoid such effects.

Fig. 7 shows the evolution of relative density and axial elastic springback for compacts produced from mixtures *1–4* as a function of compaction pressure. In mixtures *1* and *2*, which contain B_{ini}, the loading volume of boron exceeds that of titanium by factors of 2.6 and 3.6, respectively (Table 2). Therefore, curves *1*, 2 and *5*, *6* are governed primarily by the elastic properties of the starting boron powder. When the volume fraction of boron is reduced in mixtures *3* and *4* (50/50 and 58/42, respectively), the mixtures can be consolidated to higher relative densities, $\Theta_p = 0.8$.

A sample calculation of the component loading volumes for mixture *1* is shown below:

- mass of Ti powder in 100 g of mixture: 69 g;
- bulk density of Ti_{ini} (Θ_{Ti}): $0.32 \cdot 4.5 = 1.44$ g/cm^3 (4.5 g/cm^3 is the density of Ti);
- titanium volume (V_{Ti}) in 100 g of mixture: 69 g / 1.44 g/cm^3 = 47.9 cm^3;
- mass of boron powder in 100 g of mixture (Ti + 2B): 31 g;
- bulk density of B_{ini} (Θ_B): $0.14 \cdot 1.8 = 0.25$ g/cm^3 (1.8g/cm^3 is the density of amorphous boron);
- boron volume (V_B) in 100 g of mixture *1*: 31 g / 0.25 g/cm^3 = 124 cm^3;
- volume ratio B/Ti in 100 g of mixture: VB/VTi = = 124 / 47.9 ≈ 2.6;
- ratio of the volume fractions of the components (B/Ti) in the mixture: 72/28 %.

The calculated values for mixtures *2–4* are presented in Table 2.

The shape of the elastic springback curves for mixtures *1* and *2* (curves *5*, *6* in Fig. 7), where one of the components is B_{ini}, indicates that elastic deformation dominates across the entire pressure range, and the plastic deformation stage is essentially absent.

Table 2. **Characteristics of mixtures *1–4***

Таблица 2. **Характеристики смесей *1–4***

Mixture No.	Composition	Θ_{Ti}, g/cm^3	Θ_B, g/cm^3	V_B/V_{Ti}	B/Ti, vol. %
1	$Ti_{ini} + 2B_{ini}$	1.44	0.25	2.6	72/28
2	$Ti_{MA} + 2B_{ini}$	2.03	0.25	3.6	78/22
3	$Ti_{ini} + 2B_{MA}$	1.44	0.67	1.0	50/50
4	$Ti_{MA} + 2B_{MA}$	2.03	0.67	1.4	58/42

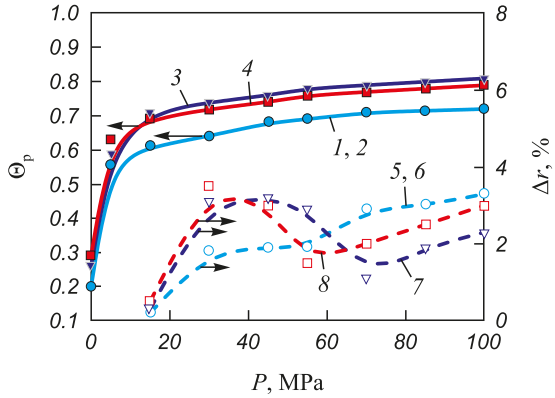

Fig. 7. Dependence of relative density (***1–4***) and axial elastic springback (***5–8***) on the compaction pressure for Ti + 2B mixtures
1, ***5*** – $Ti_{ini} + 2B_{ini}$; ***2***, ***6*** – $Ti_{MA} + 2B_{ini}$;
3, ***7*** – $Ti_{ini} + 2B_{MA}$; ***4***, ***8*** – $Ti_{MA} + 2B_{MA}$

Рис. 7. Зависимости относительной плотности (***1–4***) и упругого последействия (***5–8***) для прессовок из смесей Ti + 2B от давления прессования
1, ***5*** – $Ti_{ini} + 2B_{ini}$; ***2***, ***6*** – $Ti_{MA} + 2B_{ini}$;
3, ***7*** – $Ti_{ini} + 2B_{MA}$; ***4***, ***8*** – $Ti_{MA} + 2B_{MA}$

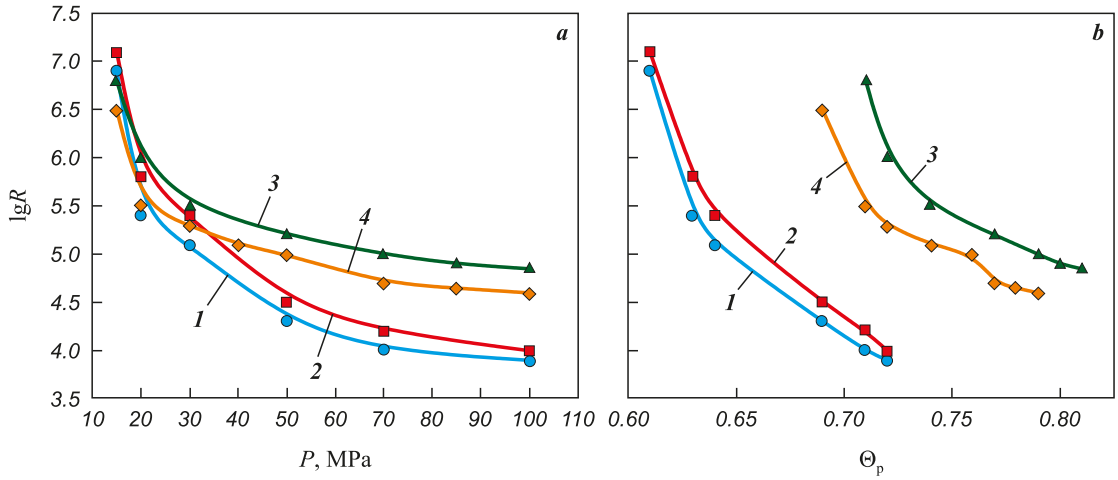

Рис. 8. Зависимости удельного электросопротивления от давления прессования (***a***) и относительной плотности смесей Ti + 2B *1–4* (***b***)

Fig. 8. Dependence of specific electrical resistivity on compaction pressure (***a***) and relative density of Ti + 2B mixtures *1–4* (***b***)

When B_{MA} is used, a decrease in Δr is observed at P = 50–70 MPa (Fig. 7), which can be interpreted as the onset of the plastic deformation stage. In this pressure interval, plastic deformation can occur only in boron particles, because the yield strength of titanium lies above 85 MPa (Fig. 5). At pressures above 30 MPa (Fig. 6), B_{MA} particles exhibit limited plasticity and may act as a lubricant during the compaction of larger titanium particles. Mixtures containing B_{MA} can be consolidated to higher relative densities, Θ_p = 0.7–0.8 (Fig. 7). This conclusion is supported by electrical resistivity measurements. As seen in Fig. 8, *b*, samples compacted from mixtures *3* and *4* exhibit higher electrical resistivity at higher densities compared with those made from mixtures *1* and *2*. This behavior is likely associated with the ability of boron – after acquiring limited plasticity as a result of mechanical activation – to spread between titanium particles at pressures above 30 MPa, thereby suppressing the growth of the Ti–Ti contact area.

Combustion of Ti + 2B mixtures

Previous studies [12; 13] have shown that the combustion temperature of Ti + 2B mixtures depends on the reaction-interface area between the starting components Ti and B: the larger the interparticle contact area, the higher the temperature within the combustion wave. The maximum attainable contact area is limited by the specific surface area of the coarser component – in this case, titanium powder (S_{sp} = 0.4–0.6 m^2/g). Therefore, the higher the specific surface area of the titanium powder, the larger the Ti–B reaction interface and the higher the combustion temperature. The reaction-interface area also depends on the density of the compacted mixtures. However, as shown in [12; 13], increasing density enhances combustion temperature only until the Ti–Ti contact area begins to grow rapidly; this enhanced heat dissipation from the reaction zone may lower the combustion temperature.

Figure 9 shows the dependence of combustion temperature and combustion-wave velocity on the relative density (Θ_p) of samples compacted from mixtures *1–4*. Samples produced from mixtures *3* and *4*, which contain B_{MA}, burn at higher temperatures ($T_{max} \approx 2800 \div 2900$ °C) The maxima of for mixtures containing B_{MA} (curves *3* and 4) occur at higher densities (Θ_p = 0.72 and 0.74) compared with mixtures containing B_{ini} (Θ_p = 0.64, curves *1* and *2*). The rise in T_c to its maximum value results from the increased Ti–B contact area with increasing density. The decrease in T_c beyond the maximum coincides, for all mixtures, with a drop in electrical resistivity below $R \approx 10^5$ Ω·cm, which indicates intensive growth of the Ti–Ti contact area (see Fig. 8). The maximum combustion temperatures for mixtures *1–4* correspond to resistivity values $\lg R \approx 5.0 \div 5.5$; at lower values of R, T_c decreases.

Fig. 9, *b* shows the combustion-wave velocities. The maxima of T_c and U_c for mixtures *3* and *4* occur at different density values, whereas for mixtures *1* and *2* both maxima coincide at Θ_p = 0.64. In the density interval $\Theta_p = 0.56 \div 0.70$, compacts *1* and *2* burn with higher velocities (9.5–10 cm/s) than compacts *3* and *4* (4.8–5.5 cm/s), which correspond to a higher density interval Θ_p (0.6–0.78).

The combustion-wave velocity is strongly affected by the conditions of off-gas escape. Increasing the com-

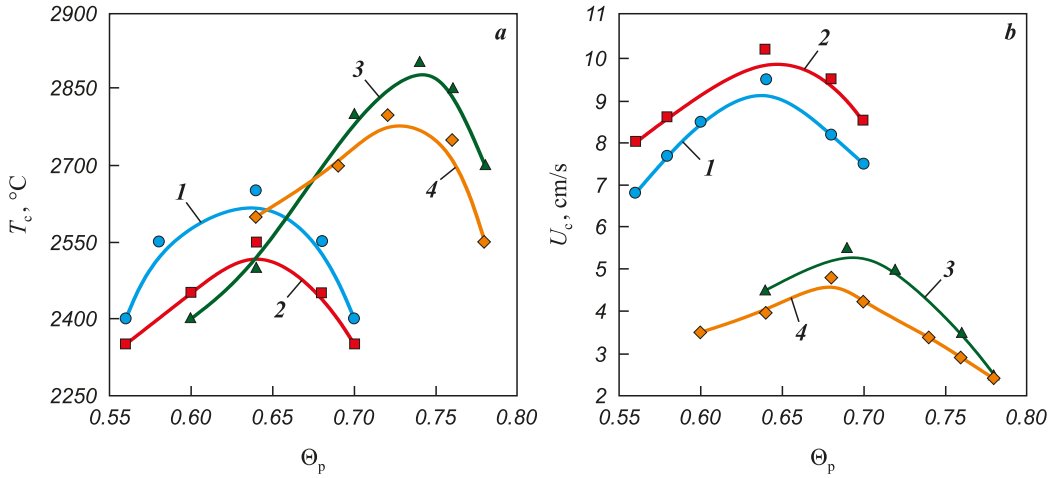

Fig. 9. Dependence of combustion temperature and combustion-wave velocity (***a***) on the relative density of samples compacted from mixtures *1–4* (***b***)

Рис. 9. Зависимости температуры и скорости горения (***a***) от относительной плотности образцов, спрессованных из смесей *1–4* (***b***)

pact density hinders removal of impurity gases released in the combustion wave, thereby reducing the combustion-wave velocity.

Discussion of results

The results demonstrate a pronounced dependence of the combustion parameters of Ti + 2B powder compacts on the conditions used for preparing the charge. The combustion temperature and combustion-wave velocity are critically important for controlling the SHS-compaction process, which ultimately governs the microstructure and properties of the resulting TiB_2 ceramic. The higher the combustion temperature – and, consequently, the temperature during hot pressing – the denser and more refined the microstructure of the TiB_2 ceramic obtained. The maximum attainable reaction-interface area between titanium and boron particles, which determines the combustion temperature, depends primarily on the specific surface area of the titanium powder. The larger this surface area, the greater the Ti–B reaction interface and the higher the combustion temperature that can be achieved during synthesis.

Mechanical activation of titanium powder in a ball mill, as shown earlier (Fig. 2), reduces its specific surface area and therefore can only decrease the combustion temperature. Thus, to achieve synthesis conditions that ensure the maximum combustion temperature, the mixing of titanium and boron powders in a ball mill must be performed under “mild” conditions, with minimal interaction between titanium and the milling media, while still ensuring homogeneous distribution of components within the mixture.

In contrast, mechanical activation of boron powder leads to the destruction of the arch-like packing structure, fragmentation of agglomerates, more homogeneous distribution of boron particles among titanium particles (as confirmed by electrical resistivity measurements, Fig. 8), and an increase in the reaction-interface area between the reactants. During compaction, B_{MA} particles act as a lubricant, allowing the charge compacts to reach relative densities of 0.70–0.75 without a significant increase in the Ti–Ti contact area ($\lg R \approx 5.0 \div 5.5$). For this reason, preliminary mechanical activation of boron before mixing with titanium yields a positive effect by increasing the combustion temperature.

The dependencies of combustion temperature and combustion-wave velocity on compact density (Fig. 9) show distinct maxima. For mixtures *1* and *2* containing B_{ini}, T_c maximum is reached at $\Theta_p = 0.64$, whereas for mixtures *3* and *4* the maxima occur at $\Theta_p = 0.72–0.74$. The electrical resistivity of the charge compacts at the combustion temperature maxima corresponds to $\lg R \approx 5.0 \div 5.5$ (Figs. 8 and 9), indicating identical Ti–Ti contact areas for all mixtures at these points. Mixtures *3* and *4*, at the same Ti–Ti contact area as mixtures *1* and 2 (as indicated by $\lg R \approx 5.0 \div 5.5$), but at higher density, likely possess a larger Ti–B reaction-interface area. Thus, maximum combustion temperatures are achieved at elevated Ti–B contact area and minimal Ti–Ti contact area. When the Ti–Ti contact area increases and the electrical resistivity drops below 10^5 Ω·cm, the combustion temperature decreases (Fig. 9, *a*). This decrease may be caused by enhanced heat removal from the reaction front, as well

as impeded off-gas evacuation due to increased compact density and the formation of closed porosity.

The combustion-wave velocity is an important technological parameter in SHS-compaction because it defines the available time window for initiating hot pressing. It was shown in [23] that U_c depends mainly on the off-gas removal conditions and only weakly on the combustion temperature (Fig. 9). The results of the present work confirm this conclusion. Although mixtures *3* and *4* exhibit higher combustion temperatures ($T_c^{max} \approx 2800$ and 2900 °C), their maximum combustion-wave velocities ($U_c^{max} \approx 4.8$ and 5.5 cm/s) are lower than those of mixtures *1* and *2* ($U_c^{max} \approx 9.5$ and 10.2 cm/s at $T_c^{max} \approx 2650$ and 2550 °C). This behavior is most likely related to the higher density of the compacts, which hinders the escape of impurity gases and therefore reduces the combustion-wave velocity. A critical density of about 0.8 was identified: compacted mixtures *3* and *4* with densities of 0.8 and higher could not be ignited.

Conclusions

1. It has been shown that preliminary mechanical activation of titanium and boron powders has a pronounced effect on the densification behavior and combustion characteristics of Ti + 2B mixtures. Mechanical activation reduces the specific surface area of the titanium powder, leading to a decrease in the Ti–B reaction-interface area and a corresponding reduction in the combustion temperature.

2. Mechanical activation of boron results in the destruction of its arch-like packing structure and fragmentation of its agglomerates, which increases the Ti–B reaction-interface area and raises the combustion temperature within the reaction front.

3. It was established that, at compaction pressures above 30 MPa, B_{MA} exhibits limited plasticity, which enables consolidation of Ti + 2B powder mixtures to relative densities of 0.7–0.8. The use of mechanically activated boron in the reactive mixtures with titanium increased the combustion temperature to 2900 °C.

4. The dependencies of combustion temperature and combustion-wave velocity on compact density exhibit distinct maxima. For mixtures containing B_{ini}, the maximum values of U_c and T_c were achieved at a relative density of 0.64. For mixtures with B_{MA}, the T_c maxima occurred at $\Theta_b = 0.72 \div 0.74$, and the U_c maximum at $\Theta_p = 0{,}68$.

5. No direct correlation between combustion temperature and combustion-wave velocity was found. Mixtures containing B_{MA} burn at a higher temperature (≈2900 °C) but with a lower combustion-wave velocity (≈5.5 cm/s) compared with mixtures containing B_{ini}, for which $T_c^{max} \approx 2650$ °C at $U_c^{max} \approx 10.2$ cm/s. The lower velocity in mixtures with B_{MA} is likely caused by hindered filtration and removal of impurity gases at higher compact densities.

6. A correlation was observed between electrical resistivity and combustion temperature: maximum T_c values correspond to a resistivity range of $R \approx 10^{5.0} – 10^{5.5}$ Ω·cm. A further decrease in resistivity below this range – associated with an increase in the Ti–Ti contact area – results in a reduction in the combustion temperature.

References / Список литературы

1. Munro R.G., Material properties of titanium diboride. *Journal of Research of the National Institute of Standards and Technology*. 2000;105(5):709–720. https://doi.org/10.6028/jres.105.057
2. Murthy T.S.R.Ch., Sonber J.K., Sairam K., Bedse R., Chakarvartty J. Development of refractory and rare earth metal borides & carbides for high temperature applications. *Materials Today: Proceedings*. 2016;3(9B):3104–3113. https://doi.org/10.1016/j.matpr.2016.09.026
3. Raju G.B., Basu B., Development of high temperature TiB_2-based ceramics. *Key Engineering Materials*. 2008;395:89–124. https://doi.org/10.4028/www.scientific.net/KEM.395.89
4. Mukhopadhyay A., Raju G.B., Basu B., Suri A.K., Correlation between phase evolution, mechanical properties and instrumented indentation response of TiB_2-based ceramics. *Journal of the European Ceramic Society*. 2009:29(3):505–516. https://doi.org/10.1016/j.jeurceramsoc.2008.06.030
5. Wang W., Fu Z., Wang H., Yuan R. Influence of hot-pressing sintering temperature and time on microstructure and mechanical properties of TiB_2 ceramics. *Journal of the European Ceramic Society*. 2002;22(7):1045–1049. https://doi.org/10.1016/S0955-2219(01)00424-1
6. Mroz C. Titanium diboride. *American Ceramic Society Bulletin*. 1995;74(6):158–159.
7. Cheloui H., Zhang Z., Shen X., Wang F., Lee S. Microstructure and mechanical properties of TiB–TiB_2 ceramic matrix composites fabricated by spark plasma sintering. *Materials Science and Engineering: A*. 2011;528(10-11):3849–3853. https://doi.org/10.1016/j.msea.2011.01.096
8. Merzhanov A.G. Solid-State Combustion. Chernogolovka: ISMAN, 2000. 224 p. (In Russ.).

   Мержанов А.Г. Твердопламенное горение. Черноголовка: ИСМАН, 2000. 224 с.
9. Pityulin A.N. Power compaction in SHS processes. In: *Selfpropagating high-temperature synthesis: Theory and practice*. Chernogolovka: Territoriya, 2001. P. 333–353. (In Russ.).

   Питюлин А.Н. Силовое компактирование в СВС процессах. В сб. науч. статей: *Самораспространяющийся*

высокотемпературный синтез: Теория и практика. Черноголовка: Территория, 2001. С. 333–353.

10. Akopyan A.G., Dolukhanyan S.K., Borovinskaya I.P. Interaction of titanium, boron and carbon in the combustion mode. *Fizika goreniya i vzryva*. 1978;(3):70–75. (In Russ.).

Акопян А.Г., Долуханян С.К., Боровинская И.П. Взаимодействие титана, бора и углерода в режиме горения. *Физика горения и взрыва*. 1978;(3):70–75.

11. Azatyan T.S., Maltsev V.M., Merzhanov A.G., Seleznev V.A. On the mechanism of propagation of the combustion wave in mixtures of titanium with boron. *Fizika goreniya i vzryva*. 1980;16(2):37–42. (In Russ.).

Азатян Т.С., Мальцев В.М., Мержанов А.Г., Селезнев В.А. О механизме распространения волны горения в смесях титана с бором. *Физика горения и взрыва*. 1980;16(2):37–42.

12. Lepakova O.K., Raskolenko L.G., Maksimov Yu.M. Investigation of titanium boride phases obtained by self-propagating high-temperature synthesis. *Neorganicheskie materialy*. 2000;36(6):690–697. (In Russ.).

Лепакова О.К., Расколенко Л.Г., Максимов Ю.М. Исследование боридных фаз титана, полученных методом самораспространяющегося высокотемпературного синтеза. *Неорганические материалы*. 2000;36(6):690–697.

13. Ponomarev M.A., Shcherbakov V.A., Shteinberg A.S. Regularities of combustion of thin layers of titanium–boron powder mixture. *Doklady AS USSR*. 1995;340(5): 642–645. (In Russ.).

Пономарев М.А., Щербаков В.А., Штейнберг А.С. Закономерности горения тонких слоев порошковой смеси титан–бор. *Доклады АН СССР*. 1995;340(5):642–645.

14. Tavadze G.F., Shteinberg A.S. Production of advanced materials by methods of self-propagating high-temperature synthesis. Berlin, Heidelberg: Springer, 2013. 156 p. https://doi.org/10.1007/978-3-642-35205-8

15. Vadchenko S.G., Boyarchenko O.D. Burning velocity of double-layer Ti + 2B strips: Influence of clearance space. *International Journal of Self-Propagating High-Temperature Synthesis*. 2018;27(2):103–106. https://doi.org/10.3103/S1061386218020164

16. Bogatov Yu.V., Levashov E.A., Blinova T.V., Pityulin A.N. Technological aspects of obtaining compact titanium diboride by SHS. *Izvestiya. Ferrous Metallurgy*. 1994;(3):51–55. (In Russ.).

Богатов Ю.В., Левашов Е.А., Блинова Т.В., Питюлин А.Н. Технологические аспекты получения компактного диборида титана методом СВС. *Известия вузов. Черная металлургия*. 1994;(3):51–55.

17. Shcherbakov V.A., Gryadnov A.N., Sachkova N.V., Samokhin A.V. SHS-compacting of ceramic composites based on titanium and chromium borides. *Pis'ma o materialakh*. 2015;5(1):20–23. (In Russ.). https://doi.org/10.22226/2410-3535-2015-1-20-23

Щербаков В.А., Грядунов А.Н., Сачкова Н.В., Самохин А.В. СВС-компактирование керамических композитов на основе боридов титана и хрома. *Письма о материалах*. 2015;5(1):20–23. https://doi.org/10.22226/2410-3535-2015-1-20-23

18. Bogatov Yu.V., Barinov V.Yu., Shcherbakov V.A. Influence of titanium powder morphology on SHS parameters and structure of compact titanium diboride. *Perspektivnye materialy*. 2020;(3):50–60. (In Russ.). https://doi.org/10.30791/1028-978X-2020-3-50-60

Богатов Ю.В., Баринов В.Ю., Щербаков В.А. Влияние морфологии порошков титана на параметры СВС и структуру компактного диборида титана. *Перспективные материалы*. 2020;(3):50–60. https://doi.org/10.30791/1028-978X-2020-3-50-60

19. Bogatov Yu.V., Shcherbakov V.A., Boyarchenko O.D. Preparation of dense TiB_2 by forced self-propagating high-temperature synthesis compaction with mechanical activation of reagents. *Inorganic Materials*. 2021;57(10):1061–1066. https://doi.org/10.1134/S0020168521100010

Богатов Ю.В., Щербаков В.А., Боярченко О.Д. Получение плотного TiB_2 методом силового СВС-компактирования с использованием механической активации реагентов. *Неорганические материалы*. 2021;57(10):1122–1127. https://doi.org/10.31857/S0002337X21100018

20. Levashov E.A., Rogachev A.S., Kurbatkina M., Yukhvid V.I. Perspective materials and technologies of self-propagating high-temperature synthesis. Moscow: MISIS, 2011. 378 p. (In Russ.).

Левашов Е.А., Рогачев А.С., Курбаткина М., Юхвид В.И. Перспективные материалы и технологии самораспространяющегося высокотемпературного синтеза. М.: Изд. дом МИСИС, 2011. 378 с.

21. Kiparisov S.S., Libenson G.A. Powder Metallurgy. Moscow: Metallurgiya. 1991. 432 p. (In Russ.).

Кипарисов С.С., Либенсон Г.А. Порошковая металлургия. М.: Металлургия. 1991. 432 с.

22. Tsemenko V.N. Deformation of powder media. SPb: SPbSTU, 2001. 104 p. (In Russ.).

Цеменко В.Н. Деформирование порошковых сред. СПб: Изд. СПбГТУ, 2001. 104 с.

23. Bogatov Yu.V., Shcherbakov V.A. Convective combustion of a mechanically activated Ti + C mixture under forced SHS compaction. *Combustion, Explosion, and Shock Waves*. 2023;59(3):353–361. https://doi.org/10.1134/S0010508223030103

Богатов Ю.В., Щербаков В.А. Конвективное горение механоактивированной смеси Ti + C в условиях силового СВС-компактирования. *Физика горения и взрыва*. 2023;59(3):109–117.

Information about the Authors

Yuri V. Bogatov – Cand. Sci. (Eng.), Senior Researcher, Laboratory of Energy-Assisted Physicochemical Processes, Merzhanov Institute of Structural Macrokinetics and Materials Science, Russian Academy of Sciences (ISMAN)
ORCID: 0000-0002-7329-2898
E-mail: xxbroddy@gmail.com

Vladimir A. Shcherbakov – Dr. Sci. (Phys.-Math.), Head of the Laboratory of Energy-Assisted Physicochemical Processes, ISMAN
ORCID: 0000-0001-5682-3792
E-mail: vladimir@ism.ac.ru

Сведения об авторах

Юрий Владимирович Богатов – к.т.н., ст. науч. сотрудник лаборатории энергетического стимулирования физико-химических процессов, Институт структурной макрокинетики и проблем материаловедения им. А.Г. Мержанова Российской академии наук (ИСМАН)
ORCID: 0000-0002-7329-2898
E-mail: xxbroddy@gmail.com

Владимир Андреевич Щербаков – д.ф.-м.н., зав. лабораторией энергетического стимулирования физико-химических процессов, ИСМАН
ORCID: 0000-0001-5682-3792
E-mail: vladimir@ism.ac.ru

Contribution of the Authors

Yu. V. Bogatov – conceptualization, experimental work, data analysis, writing and preparation of the manuscript.
V. A. Shcherbakov – discussion of the results, contribution to manuscript writing.

Вклад авторов

Ю. В. Богатов – определение цели работы, проведение экспериментов, написание статьи.
В. А. Щербаков – участие в обсуждении результатов и написание статьи.

Received 01.03.2025
Revised 20.05.2025
Accepted 23.05.2025

Статья поступила 01.03.2025 г.
Доработана 20.05.2025 г.
Принята к публикации 23.05.2025 г.